

Flexible Operation of Batteries in Power System Scheduling with Renewable Energy

Nan Li, *Student Member, IEEE*, Canan Uckun, Emil Constantinescu, John R. Birge, Kory W. Hedman, *Member, IEEE*, and Audun Botterud, *Member, IEEE*

Abstract—The fast growing expansion of renewable energy increases the complexities in balancing generation and demand in the power system. The energy-shifting and fast-ramping capability of energy storage has led to increasing interests in batteries to facilitate the integration of renewable resources. In this paper, we present a two-step framework to evaluate the potential value of energy storage in power systems with renewable generation. First, we formulate a stochastic unit commitment approach with wind power forecast uncertainty and energy storage. Second, the solution from the stochastic unit commitment is used to derive a flexible schedule for energy storage in economic dispatch where the look-ahead horizon is limited. Analysis is conducted on the IEEE 24-bus system to demonstrate the benefits of battery storage in systems with renewable resources and the effectiveness of the proposed battery operation strategy.

Index Terms—Battery, economic dispatch, energy storage, flexible resources, integer programming, power system economics, power system reliability, real-time operation, renewable resources, stochastic unit commitment.

NOMENCLATURE

Indices and Sets

b :	Index of energy storage units.
e :	Index of “buckets” used in stochastic unit commitment.
g :	Index of generators.
i :	Number of look-ahead time periods in the hourly-dispatch model.
k :	Index of transmission lines.
n :	Index of buses.
s :	Index of scenarios.
t :	Index of time periods.
t' :	Current time period in the hourly-dispatch model.
w :	Index of wind farms.
$\delta_k^+(n)$:	For any transmission line k with “to” bus n .
$\delta_k^-(n)$:	For any transmission line k with “from” bus n .

Supported by the University of Chicago and the Department of Energy under DOE Contract No. DE-AC02-06CH11357 awarded to UChicago Argonne, LLC, operator of Argonne National Laboratory, and by the Power Systems Engineering Research Center (PSERC).

Nan Li and Kory W. Hedman are with Arizona State University, Tempe, AZ 85287 USA. E-mail: {nanli4, khedman}@asu.edu.

Canan Uckun, Emil Constantinescu, and Audun Botterud are with Argonne National Laboratory, Lemont, IL 60439 USA. E-mail: {cuckun, emconsta, abotterud}@anl.gov.

John R. Birge is with the University of Chicago, Chicago, IL 60637 USA. E-mail: jbirge@chicagobooth.edu.

Ω_{Gs} :	Set of slow generators.
$\forall(n)$:	For any generating unit at bus n .
<i>Parameters</i>	
B_k :	Susceptance of line k .
$C_g(x)$:	Variable cost function for generator g .
c_{bt}^{Low} :	Cost for violating the lower bound of the flexible operating range for energy storage b in time period t .
c_g^{NL} :	No-load cost for generator g .
c_g^{SU} :	Startup cost for generator g .
c_{bt}^{Up} :	Cost for violating the upper bound of the flexible operating range for energy storage b in time period t .
c^{vL} :	Cost for involuntary load shedding.
c^{vOR} :	Cost for violating the system operating reserve (sum of spinning and non-spinning) requirement.
c^{vR+}, c^{vR-} :	Cost for violating the system up and down regulation reserve requirement.
c^{vSP} :	Cost for violating the system spinning reserve requirement.
d_{nt} :	Real power demand at node n in time period t .
DT_g :	Minimum down time for unit g .
E_{bt}^{Low} :	Lower bound of the flexible operating range for energy storage b in time period t .
E_b^{Min} :	Minimum energy capacity for energy storage b .
E_b^{Max} :	Maximum energy capacity for energy storage b .
E_{bt}^{Up} :	Upper bound of the flexible operating range for energy storage b in time period t .
$P_b^{In_max}$:	Maximum power absorption for energy storage b .
$P_b^{Out_max}$:	Maximum power output for energy storage b .
P_g^{Max} :	Maximum real power output for generator g .
P_g^{Min} :	Minimum real power output for generator g .
P_k^{max} :	Maximum active power capacity for line k .
P_{wst}^{Wind} :	Generation for wind farm w in time period t and scenario s .
R_g^{60+} :	Maximum hourly ramp up rate for generator g .
R_g^{60-} :	Maximum hourly ramp down rate for generator g .
R_g^{10+} :	Maximum 10-min ramp up rate for generator g .
R_g^{5+} :	Maximum 5-min ramp up rate for generator g .
R_g^{5-} :	Maximum 5-min ramp down rate for generator g .
R_g^{SD} :	Maximum shut down ramp rate for generator g .
R_g^{SU} :	Maximum start up ramp rate for generator g .
R_g^{NS} :	Maximum non-spinning reserve ramp rate for generator g .
Q_{st}^{OR} :	System operating reserve requirement in time

\bar{u}_{gt} :	period t and scenario s . Unit commitment status for generator g (0 down, 1 online), which is obtained from the day-ahead solution.
UT_g :	Minimum up time for unit g .
α_b^R :	Minimum duration of time (hour) that the regulation reserves have to be maintained.
α_b^S :	Minimum duration of time (hour) that the spinning reserves have to be maintained.
η_b^{In} :	Efficiency associated with the absorbing cycle for energy storage b .
η_b^{Out} :	Efficiency associated with the generating cycle for energy storage b .
π_s :	Probability for scenario s .
<i>Decision Variables (Index s Denotes Scenario and Index t Denotes Time Period)</i>	
E_{bst} :	State of charge for energy storage b .
P_{gst} :	Power output for generator g .
P_{bst}^{In} :	Power absorbed by energy storage b .
P_{bst}^{Out} :	Power generated by energy storage b .
P_{kst} :	Real power flow on transmission line k .
r_{gst}^S :	Spinning reserve provided by generator g .
r_{gst}^{R+} :	Up regulation reserve provided by generator g .
r_{gst}^{R-} :	Down regulation reserve provided by generator g .
r_{gst}^{NS} :	Non-spinning reserve provided by generator g .
S_{nst}^L :	Involuntary load shedding at node n .
$S_{b,t}^{Low}$:	Slack variable to relax the lower bound of the flexible operating range for energy storage b .
S_{st}^{R+} :	Slack variable to relax system up regulation requirement.
S_{st}^{R-} :	Slack variable to relax system down regulation requirement n .
S_{st}^{SP} :	Slack variable to relax system spinning reserve requirement.
S_{st}^{OR} :	Slack variable to relax system operating reserve requirement.
$S_{b,t}^{Up}$:	Slack variable to relax the upper bound of the flexible operating range for energy storage b .
S_{wst}^W :	Wind curtailment for wind farm w .
u_{gst} :	Binary unit commitment variable for generator g (0 down, 1 online).
v_{gst} :	Startup variable for generator g (1 for startup, 0 otherwise).
w_{gst} :	Shutdown variable for generator g (1 for shutdown, 0 otherwise).
z_{bst} :	Binary variable for energy storage b (1 for production, 0 for consumption).
θ_{kst}^+ :	Bus angle for the “from” bus of transmission line k .
θ_{kst}^- :	Bus angle for the “to” bus of transmission line k .

I. INTRODUCTION

WITH increasing concerns about climate change and the need for a more sustainable grid, power systems have seen a fast expansion of renewable resources in recent years. The variability and uncertainty of renewable resources

have increased the complexities in balancing load with generation and have introduced new challenges in regards to maintaining system reliability. As a result, more flexible resources are needed to meet the increasingly stringent ramping requirements in the system.

Driven by the need to integrate higher penetration levels of renewable energy and to reduce the costs for serving peak demands, recent interests have been focused on energy storage technologies. Energy storage can shift energy from peak-demand hours to off-peak-demand hours, or absorb excess renewable energy to provide it back to the grid when desired. The fast-ramping capability also makes energy storage a competitive resource to compensate for the variability and uncertainty in renewable energy. By using energy storage, the cycling of thermal units can be reduced, which is an advantage since many thermal units are not designed to be ramped up and down frequently [1].

Among all existing storage technologies, there is substantial interest in batteries as an emerging solution to manage intermittent renewable resources. Compared with thermal units, batteries do not have a no-load cost and they are generally considered to not have minimum power input/output levels for charging/discharging. Compared to other storage technologies, such as pumped storage hydro and compressed air energy storage, batteries have higher power density. Even though the main barrier with battery technologies is their high capital costs, efforts are being made to reduce the capital costs and improve the cost-effectiveness of different battery solutions [2].

Due to growing interests in energy storage, recent literature analyzes the scheduling problem of energy storage and the different applications of energy storage in systems with increased renewable resources [3]-[8]. The application of battery storage is studied at both the transmission and distribution system levels. In [9] and [10], the authors studied the benefits of batteries in transmission systems with renewable resources using security-constrained unit commitment (UC) models. In [11] and [12], the application of battery storage at the distribution level is studied. In [11], the benefits of using battery storage in microgrids with renewable resources are evaluated using a three-step short-term generation scheduling approach. In [12], a unit commitment model is formulated to study the problem of battery optimal sizing in a microgrid system.

While the study of battery storage in systems with renewable resources is not new, much of the previous work is based on day-ahead models or short-term look-ahead scheduling models [9]-[12]. In such look-ahead scheduling problems, scheduling for future time periods are optimized together in one model based on forecast information. However, with a look-ahead type of scheduling model, the challenges associated with managing the state of charge (SOC) of the battery are not properly captured. Different from thermal units, the dispatch of energy storage is constrained by their SOC. In real-time operation, as look-ahead functionality is limited, decisions for time period t have to be made in advance without having perfect information about future uncertainties. An inappropriate decision made for battery storage in the current time period could potentially result in insufficient capacity to charge or discharge in future time

periods. These challenges are not adequately captured in independent day-ahead or short-term look-ahead scheduling models.

In this paper, we study battery storage under the assumption that it is a system asset operated by the system operator. We propose a two-step modeling framework to study the benefit and the operation of battery storage in transmission systems with renewable generation. The main contributions of the paper are as follows. Firstly, we propose a flexible operational strategy for the use of energy storage in real-time operations. The proposed approach is developed to utilize the flexibility of battery storage across multiple time periods, given the limited look-ahead functionality and future uncertainty in real-time operation. Secondly, we extend the work in [13] to include energy storage. While the primary motivation for [13] is to propose an improved stochastic formulation to enhance the flexibility of the commitment schedule for thermal generators, we extend the formulation in [13] and take the advantage of its structure to develop the proposed battery operational scheme in this paper. Thirdly, we illustrate the benefits of the proposed algorithms in a case study of the IEEE RTS system using realistic wind power uncertainty data.

This paper is different from previous studies as follows. While stochastic UC models have been used to study battery storage and other forms of energy storage in [9]-[12], [14]-[17], the studies in [9]-[12], [14]-[17] are conducted using day-ahead or short-term look-ahead scheduling models. None of [9]-[12], [14]-[17] addresses the challenges associated with the real-time operation of energy storage. In [18]-[20], different methodologies are used to improve the operational scheme of the battery in real-time operation. However, the studies in [18]-[20] are conducted from the viewpoint of the storage owner, whose objective is to maximize his/her own profit. In this paper, the study is conducted from the viewpoint of a system operator, whose objective is to optimally allocate the resources in the system and minimize the total cost of the system. In [21], an energy restoration mechanism is proposed to maintain the SOC of energy storage at their preferred levels. The approach in [21] is proposed to manage the SOC of energy storage when energy storage is used to provide regulation reserve. However, in this paper, the proposed approach is to improve the overall operational scheme of battery storage in real-time operation, rather than focusing on any one type of ancillary services provided by the battery.

The remainder of the paper is organized as follows. In Section II, the mathematical model and the methodology are described. The results are reported and discussed in Section III. The conclusion and future work are presented in Section IV.

II. MATHEMATICAL MODEL AND METHODOLOGY

A two-step framework is implemented to evaluate the benefits of battery storage in transmission systems with renewable generation. In the first-step, which is referred to as the day-ahead scheduling, a two-stage stochastic day-ahead unit commitment model is formulated. In the second-step, stochastic simulation is performed to test the day-ahead solution against wind scenarios that are not included in the day-ahead stochastic UC. The second-step is later referred to

as the post-stage analysis. The formulation used in the two-step framework is described in the following subsections.

A. Day-Ahead Scheduling and Stochastic Unit Commitment

The stochastic UC is formulated as a mixed integer linear program (MILP) based on the formulation in [13]. In [13], the scheduling horizon is divided into several time blocks. Within each time block, wind scenarios are grouped into different “buckets” based on their average wind forecast value. The non-anticipativity constraints are then enforced for scenarios that are in the same bucket in each time block. The advantage of this formulation is that it can provide a more flexible schedule for the thermal generators as the commitment schedule is dependent on each bucket rather than being the same for all the scenarios in the stochastic UC. It should be noted that the day-ahead UC model is still solved for the full 24-hour time horizon. The introduction of time blocks is primarily to introduce flexibility in the solution by allowing commitment decisions for thermal units to vary between buckets and time blocks, as a function of the wind power level.

The complete formulation of the stochastic UC with energy storage is presented in (1) - (29), where the objective (1) is to minimize the system total costs and the costs of security violations (e.g., the cost of involuntary load shedding and violations of the reserve requirements). In the formulation, constraint (2) guarantees the power balance at every bus. Constraint (3) represents the dc power flow on each line and (4) is the line-flow limit constraint. Limits on the power output for each generator are presented in (5) and (6). The non-anticipativity constraints are shown in (7), where e is the index for buckets. In constraint (7), $e = \beta(s, t)$ indicates that scenario s is assigned to bucket e in time period t . Note that the non-anticipativity constraints are only modeled for the slow units and enforced for each individual bucket, i.e. not across all the scenarios. The minimum up and down time constraints are shown in (8)-(10). Constraints (11)-(14) represent the ramp rates for regulation, spinning and non-spinning reserves for thermal units. In this paper, regulation reserve refers to the reserve that is used to follow the automatic generation control (AGC) signal. For spinning and non-spinning reserves, they are modeled to represent contingency reserve, which is used to respond to contingencies in the system. The hourly ramp rate constraints are shown in (15) and (16). The model for battery is shown in (17)-(24). Constraints (17)-(20) represent the limits on regulation and spinning reserves provided by batteries. Constraints (18) and (20) indicate that a battery should be able to maintain its output for duration of α_b^S and α_b^R hours to be qualified to provide spinning and regulation reserves respectively. Constraint (21) is the power balance constraint for energy storage. Regulation reserve variables are included in (21) to estimate the change in SOC as a result of the deployment of the regulation reserves. We ignore the impact of the wind penetration level on the requirement for regulation reserves, and assume that 20% of the scheduled regulation reserve capacity will be activated regardless of the wind penetration levels studied. The limits on consumption and production for the battery are presented in (22) and (23). Constraint (24) represents the energy capacity for the battery. The constraints

for system-wide regulation and spinning reserve requirements are presented in (25)-(29). In the paper, the regulation reserve requirement is set to be 2% of the load, while the operating reserve (sum of spinning and non-spinning reserve) is required to be greater or equal to the single largest generator contingency. It is also required that half of the system operating reserve should come from spinning reserve. The reserves needed to compensate renewable uncertainties are addressed endogenously by the stochastic UC model. The reserve requirement constraints can be violated for a predetermined penalty price, as reflected in the objective function.

Minimize:

$$\begin{aligned} \sum_s \pi_s \{ & \sum_g \sum_t [C_g(P_{gst}) + c_g^{NL} u_{gst} + c_g^{SU} v_{gst}] + \\ & \sum_n \sum_t c^{VL} s_{nst}^L + \sum_t (c^{VR+} s_{st}^{R+} + c^{VR-} s_{st}^{R-} + c^{VSP} s_{st}^{SP} + \\ & c^{VOR} s_{st}^{OR}) \} \end{aligned} \quad (1)$$

Subject to:

$$\sum_{\forall g(n)} P_{gst} + \sum_{k \in \delta^+(n)} P_{kst} - \sum_{k \in \delta^-(n)} P_{kst} + \sum_{\forall b(n)} (P_{bst}^{out} - P_{bst}^{in}) = d_{nt} - s_{nst}^L - \sum_{\forall w(n)} (P_{wst}^{Wind} - s_{wst}^W), \forall n, t, s \quad (2)$$

$$P_{kst} - B_k(\theta_{kst}^+ - \theta_{kst}^-) = 0, \forall k, t, s \quad (3)$$

$$-P_k^{max} \leq P_{kst} \leq P_k^{max}, \forall k, t, s \quad (4)$$

$$P_{gst} + r_{gst}^{R+} + r_{gst}^S \leq P_g^{max} u_{gst}, \forall g, t, s \quad (5)$$

$$P_g^{min} u_{gst} \leq P_{gst} - r_{gst}^{R-}, \forall g, t, s \quad (6)$$

$$u_{gst} = u_{get}, \forall g \in \Omega_{GS}, t, e = \beta(s, t), s \quad (7)$$

$$\sum_{q=t-UT_g+1}^t v_{gsq} \leq u_{gst}, \forall g, t \in \{UT_g, \dots, T\}, s \quad (8)$$

$$\sum_{q=t-DT_g+1}^t w_{gsq} \leq 1 - u_{gst}, \forall g, t \in \{DT_g, \dots, T\}, s \quad (9)$$

$$v_{gst} - w_{gst} = u_{gst} - u_{g,s,t-1}, \forall g, t, s \quad (10)$$

$$r_{gst}^{R+} \leq R_g^{5+} u_{gst}, \forall g, t, s \quad (11)$$

$$r_{gst}^{R-} \leq R_g^{5-} u_{gst}, \forall g, t, s \quad (12)$$

$$r_{gst}^S \leq R_g^{10+} u_{gst}, \forall g, t, s \quad (13)$$

$$r_{gst}^{NS} \leq R_g^{NS} (1 - u_{gst}), \forall g, t, s \quad (14)$$

$$P_{g,s,t} - P_{g,s,t-1} \leq R_g^{60+} u_{g,s,t-1} + R_g^{SU} v_{gst}, \forall g, t, s \quad (15)$$

$$P_{g,s,t-1} - P_{g,s,t} \leq R_g^{60-} u_{gst} + R_g^{SD} w_{gst}, \forall g, t, s \quad (16)$$

$$r_{bst}^S + r_{bst}^{R+} \leq P_b^{out_max} - P_{bst}^{out} + P_{bst}^{in}, \forall b, t, s \quad (17)$$

$$\alpha_b^S r_{bst}^S + \alpha_b^R r_{bst}^{R+} \leq \eta_b^{out} (E_{bst} - E_b^{Min}), \forall b, t, s \quad (18)$$

$$r_{bst}^{R-} \leq P_b^{in_max} - P_{bst}^{in} + P_{bst}^{out}, \forall b, t, s \quad (19)$$

$$\alpha_b^R r_{bst}^{R-} \leq (E_b^{Max} - E_{bst}) / \eta_b^{in}, \forall b, t, s \quad (20)$$

$$E_{bst} = E_{b,s,t-1} + P_{bst}^{in} \eta_b^{in} - P_{bst}^{out} / \eta_b^{out} + 0.2 \alpha_b^R (r_{bst}^{R-} \eta_b^{in} - r_{bst}^{R+} / \eta_b^{out}), \forall b, t, s \quad (21)$$

$$0 \leq P_{bst}^{out} \leq P_b^{out_max} z_{bst}, \forall b, t, s \quad (22)$$

$$0 \leq P_{bst}^{in} \leq P_b^{in_max} (1 - z_{bst}), \forall b, t, s \quad (23)$$

$$E_b^{Min} \leq E_{bst} \leq E_b^{Max}, \forall b, t, s \quad (24)$$

$$\sum_g r_{gst}^{R+} + \sum_b r_{bst}^{R+} \geq 0.02 \sum_n d_{nt} - s_{st}^{R+}, \forall t, s \quad (25)$$

$$\sum_g r_{gst}^{R-} + \sum_b r_{bst}^{R-} \geq 0.02 \sum_n d_{nt} - s_{st}^{R-}, \forall t, s \quad (26)$$

$$Q_{st}^{OR} \geq P_{gst} + r_{gst}^S, \forall g, t, s \quad (27)$$

$$\sum_g r_{gst}^S + \sum_b r_{bst}^S + \sum_g r_{gst}^{NS} \geq Q_{st}^{OR} - s_{st}^{OR}, \forall t, s \quad (28)$$

$$\sum_g r_{gst}^S + \sum_b r_{bst}^S \geq 0.5 Q_{st}^{OR} - s_{st}^{SP}, \forall t, s \quad (29)$$

B. Post-Stage Analysis and Hourly-Dispatch Problem

In the second-step, which is referred to as the post-stage analysis, stochastic simulation is performed to test the day-ahead solution against wind scenarios that are not included in the day-ahead UC. In the post-stage analysis, only the uncertainty in renewable generation is considered; load forecast uncertainty and generator outages are not included. The post-stage analysis is formulated using an hourly-dispatch model. The complete formulation for the hourly-dispatch model is presented in (30)-(33). A deterministic formulation is used and only one scenario is included in each dispatch problem. In (30)-(33), index t' represents the current time period and i represents the number of look-ahead time periods included. Each dispatch run solves for the current hour and looks i hours ahead ($i=1$ as default assumption), for which a *persistence* wind power forecast is assumed. The objective is to minimize the total cost in the current hour and the look-ahead period, as shown in (30). The hourly dispatch problem is solved sequentially for 24 hours using a rolling window. The hourly-dispatch model is formulated to approximate the real-time operation, but with a lower time resolution than what is typically used in U.S. energy markets. The commitment schedule for slow (slow-start) units is given by the day-ahead UC, as shown in (31). Parameter \bar{u}_{gt} is the commitment status obtained from day-ahead UC. Fast (fast-start) units are allowed to change commitment status in the hourly-dispatch problem. In the paper, slow units are defined as the generators that have minimum up and down time greater than one hour. Fast units are defined as the generators that have minimum up and down time smaller or equal to one hour. A persistence wind power forecast is assumed for the look-ahead period, as shown in (33). The other constraints for the hourly-dispatch model are similar to those used in the day-ahead UC.

Minimize:

$$\sum_{t=t'}^{t'+i} \left[C_g(P_{gt}) + c_g^{NL} u_{gt} + c_g^{SU} v_{gt} \right] + \sum_n \sum_{t=t'}^{t'+i} c^{VL} s_{nt}^L + \sum_{t=t'}^{t'+i} \left(c^{VR+} s_t^{R+} + c^{VR-} s_t^{R-} + c^{VSP} s_t^{SP} + c^{VOR} s_t^{OR} \right) \quad (30)$$

Subject to:

$$u_{gt} = \bar{u}_{gt}, \forall g \in \Omega_{GS}, t \in \{t', \dots, t' + i\} \quad (31)$$

$$\text{Constraints (2)-(6), (11)-(29), } t \in \{t', \dots, t' + i\} \quad (32)$$

$$P_{wt}^{Wind} = P_{w,t-1}^{Wind}, \forall w, t \in \{t' + 1, \dots, t' + i\} \quad (33)$$

C. Battery Operation with a Fixed Operating Schedule

To address the limited look-ahead functionality in real-time operation, one approach is to use the solution obtained through a look-ahead scheduling stage. However, as the SOC is a second-stage decision in the day-ahead stochastic UC, one battery schedule is obtained for each scenario. Therefore, in

the post-stage analysis, for each wind scenario to be tested, the most appropriate battery schedule should be selected from the day-ahead solution. In this paper, the battery schedule is selected based on the similarity between the post-stage wind scenario and the day-ahead wind scenario. The similarity between the two wind scenarios is measured by the Euclidean distance. Therefore, for each post-stage wind scenario, s , the day-ahead wind scenario \bar{s}_0 that is closest to it is identified. Then the battery schedule that corresponds to scenario \bar{s}_0 is used in the post-stage scenario s . Denote this battery schedule as $\mathbf{E}_{\bar{s}_0}$, where $\mathbf{E}_{\bar{s}_0}$ is a vector with each element representing a target SOC in each time period.

For each post-stage scenario, the corresponding battery schedule has to be determined before the first time period is solved. To reflect the fact that wind generation cannot be perfectly forecasted while not over-complicating the simulation process, the wind generation profiles in the first six hours of each post-stage scenario are used to determine the closest day-ahead wind scenario. The underlying assumption is that the wind forecast for the first six hours has relatively low forecast errors and can be used as an acceptable approximation to determine which day-ahead schedule should be used. The battery schedule obtained using the above method is later referred to as the “fixed schedule” and will be used as a benchmark approach to be compared with our proposed method.

D. Battery Operation with a Flexible Operating Range

Next, we propose an approach that aims at flexibly operating battery storage in real-time operation while taking into account future uncertainties. Two goals are to be achieved by using the proposed method. First, the approach should be able to provide instructions to the battery of when to charge, discharge, and provide reserves, so that the battery will have enough capability in current as well as future time periods. Second, the proposed method should provide enough room for adjustment in real-time operation, such that the fast-ramping capability of the battery can be utilized when renewable generation deviates away from its planned production. The proposed method is referred to as the flexible operating range approach, and constitutes an improvement to the fixed-schedule approach. In the proposed method, an operating range is determined for the battery in each time period. The fundamental idea of the proposed method is to use the day-ahead UC solution to generate an operating range around the fixed schedule for the battery in real-time operation. The detailed procedure for determining the flexible operating range is described as follows.

Firstly, obtain a fixed schedule for the battery for each post-stage scenario s using the procedure described in the previous subsection. This is done prior to the beginning of the simulation for each post-stage scenario. Denote this fixed schedule as $\mathbf{E}_{\bar{s}_0}$. Secondly, prior to solving the hourly-dispatch problem for each time period, find the day-ahead scenarios that are in the same bucket as the post-stage scenario s and denote the corresponding day-ahead battery schedules as $\mathbf{E}_{\bar{s}_1}, \dots, \mathbf{E}_{\bar{s}_m}$. Then the upper and lower limit of the flexible operating range are determined as

$$E_{b,t}^{Up} = \max \{E_{\bar{s}_0,t}, E_{\bar{s}_1,t}, \dots, E_{\bar{s}_m,t}\}, \forall b, t \quad (34)$$

$$E_{b,t}^{Low} = \min \{E_{\bar{s}_0,t}, E_{\bar{s}_1,t}, \dots, E_{\bar{s}_m,t}\}, \forall b, t \quad (35)$$

$$E_{b,t}^{Low} - s_{b,t}^{Low} \leq E_{b,t} \leq E_{b,t}^{Up} + s_{b,t}^{Up}, \forall b, t \quad (36)$$

where $E_{b,t}^{Low}$ and $E_{b,t}^{Up}$ are the lower and upper bound for the flexible operating range in time period t for the battery. The flexible operating range is formulated as a pair of limits on SOC. Variables $s_{b,t}^{Low}$ and $s_{b,t}^{Up}$ are slack variables used to relax the flexible operating range when necessary by incurring a penalty cost. The penalty cost is computed as

$$\sum_b \sum_t (c_{bt}^{Low} s_{bt}^{Low} \eta_b^{Out} + c_{bt}^{Up} s_{bt}^{Up} / \eta_b^{In}). \quad (37)$$

For the proposed flexible operating range approach, the penalty cost term shown in (37) is added to the objective function of the hourly-dispatch problem (30). In this paper, c_{bt}^{Low} and c_{bt}^{Up} are both assumed to be the highest marginal costs of all the online slow units. The reason for using such a penalty price is that constraint (36) should be relaxed if it can avoid the commitment of an additional fast unit, which typically happens when all the slow units are fully dispatched. As turning on an additional fast unit will incur not only marginal fuel cost but also no-load cost and start-up cost, the commitment of an additional fast unit is expected to be more expensive than using the energy stored in the battery. The procedure to implement the proposed approach in the post-stage analysis is summarized in Fig. 1.

E. Renewable Scenario Generation

Wind power forecasts are affected by several sources of uncertainty that include data and physics modeling. In this study the wind scenarios account for the errors in the numerical weather predictions (NWP) and are generated using Gaussian process (GP) regression [23]. The GP is built to estimate the differences between a state-of-the-art NWP forecasts, WRF v3.6 [24], and observations (corresponding to NOAA Surfrad network). The NWP forecasts are initialized using North American Regional Reanalysis fields. Simulations are started every day during August 2012 and cover the continental U.S. on a grid of 25x25 Km. A GP is calibrated to reproduce the discrepancy between forecasts and observations at 10m height (mean and variance). Samples from this distribution are extrapolated from 10m to 100m hub height and passed through a standard power curve to obtain the wind scenarios for representative locations [25]. In the paper, only wind generation is considered. Other renewable resources, such as solar generation, are not considered in the study, but could also be represented in the model.

F. Experimental Setup

Firstly, wind scenarios are generated based on the approach outlined above. The scenario reduction approach in [26] is applied to select a predetermined number of scenarios to be used in the day-ahead UC. Secondly, the stochastic UC is solved with the reduced scenario set. The day-ahead solution is then tested against wind scenarios that are not included in the day-ahead UC (i.e. out-of-sample) in the post-stage analysis. In the post-stage, the scenarios have equal probabilities. Lastly, the performance of the proposed flexible operating range approach is compared with other benchmark methods.

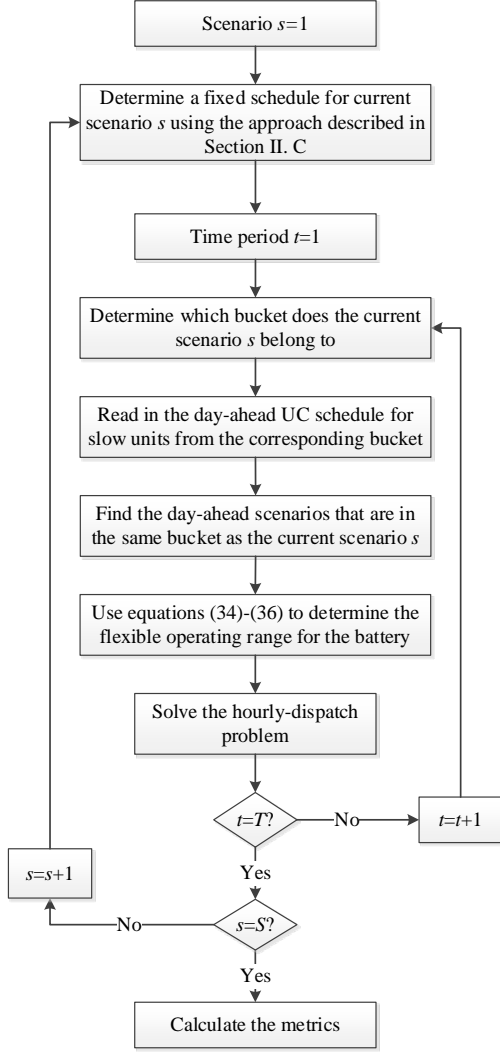


Fig. 1. Flowchart for the implementation of the proposed approach in post-stage analysis.

III. CASE STUDY

The case study is conducted on the IEEE RTS 24-bus system [27], [28]. The RTS 24-bus system has 35 branches, 32 generators, and 21 loads. The load in the system is decreased such that the peak load is 2565 MW. Similar to [29], the capacity of line (14-16) is reduced to 350 MW to create congestion in the system. One 50MW/150MWh battery unit is placed at bus 13, i.e. at the location of one of the two wind farms in the system (the second is at bus 22). Placing the battery at a wind farm location is an existing practice [30]-[32]. By installing battery storage at a wind farm location, the battery could be used to moderate the output of the wind farm. Moreover, co-location of storage and a wind farm oftentimes reduce interconnection and investment costs. The parameters used for the battery are summarized in Table I. Note that the capacity of the battery is only about 2% of the system peak load. In the day-ahead UC, an initial SOC of 90 MWh is assumed for the battery. It is required in the day-ahead UC that at the end of the day, the SOC of the battery should be the same as the initial SOC. Parameters α_b^S and α_b^R are assumed to be 0.5, which indicates that battery storage should have enough energy to maintain its output for half an hour in order to be qualified to provide spinning and regulation reserves.

TABLE I. SUMMARY OF THE PARAMETERS USED FOR BATTERY STORAGE

$\eta_b^{In}, \eta_b^{Out}$	$P_b^{In_max}, P_b^{Out_max}$ (MW)	E_b^{Min} (MWh)	E_b^{Max} (MWh)
0.9	50	30	150

Two hundred wind scenarios are generated for day 236 in 2012 and 40 scenarios are selected for the day-ahead UC for two locations in the Western United States. In the post-stage analysis, 150 scenarios are used to test the day-ahead solution. The simulation is conducted for wind penetration levels from 15% to 30%, with an increment of 5%. The wind penetration level is defined as the ratio of daily total wind generation to the daily total demand. Wind curtailment is allowed when the system cannot accommodate all of the available wind production. The cost of involuntary load shedding is assumed to be 9000 \$/MWh, and the cost for violations of reserve requirements is assumed to be 3300 \$/MWh. In the stochastic UC, the planning horizon is divided into four time blocks, with each to be six hours. In each time block, two buckets are modeled. Wind scenarios are assigned to each bucket based on their average wind generation in the corresponding time block.

A. Evaluation of the Benefits of Battery Storage

1) Day-Ahead Scheduling

In the day-ahead scheduling stage, the stochastic UC is solved. Four metrics are used to evaluate the operational benefits of battery storage, which are expected involuntary load shedding, expected wind curtailment, expected reserve requirement violations and expected total generator commitment hours (ETCH). The metric “expected reserve requirement violations” is the sum of violations of regulation and operating reserves. The metric “expected total generator commitment hours” is computed as

$$ETCH = \sum_{g,t,s} \pi_s u_{gst} \quad (38)$$

which is the weighted average of the sum of the commitment hours for all the generators in a day. If this metric is low, it means that thermal units are committed less frequently in the system. The metric ETCH is shown for slow units and fast units separately. As shown in Table II, with battery storage in the system, the ETCH for the slow units is much lower than that in the cases without battery storage. With battery storage in the system, fewer slow units are needed to address the variability in renewable resources. At the same time, the need for fast units to compensate the uncertainty in renewable generation is also slightly reduced. Meanwhile, more wind generation is dispatched in general when battery storage is included in the system due to reduced wind curtailment. The expected system total costs for the cases with and without battery storage are presented in Table III. It is shown in Table III that the system total costs are significantly reduced when battery storage is included. The day-ahead result shows that the battery is a valuable resource in helping integrate high levels of renewable resources, especially when considering that the battery in the system is relatively small compared to the system load and wind generation. As renewable penetration levels increase, the value of the flexibility that battery storage provides also increases.

TABLE II. EXPECTED SYSTEM RESULTS FOR DAY-AHEAD UNIT COMMITMENT

Wind %	Involuntary Load Shedding (MWh)	Wind Curtailment (MWh)	Reserve Violations (MWh)	ETCH for Slow Units (h)	ETCH for Fast Units (h)
With Battery					
15%	0.0	4	0.0	297	144
20%	0.0	99	0.4	282	140
25%	0.0	221	0.2	271	137
30%	0.0	1036	0.1	278	135
No Battery					
15%	0.0	5	0.3	369	144
20%	0.0	56	5.4	345	147
25%	0.0	468	4.1	331	147
30%	0.0	1460	2.9	311	146

TABLE III. EXPECTED SYSTEM TOTAL COSTS AND COST SAVINGS FOR DAY-AHEAD UNIT COMMITMENT

Wind %	Total Cost with Battery (\$)	Total Cost without Battery (\$)	Cost Savings (\$)	Cost Savings (%)
15%	806,287	930,440	124,154	13.3%
20%	765,307	887,480	122,173	13.8%
25%	733,779	849,963	116,184	13.7%
30%	712,808	827,570	114,762	13.9%

2) Post-Stage Analysis with the Fixed Operating Schedule

In the post-stage analysis, we first test the fixed-schedule approach, where the battery is not allowed to deviate from the schedule. The same metrics used in the day-ahead scheduling stage are used in the post-stage analysis. The results for post-stage analysis are reported in Table IV and Table V. From Table IV and Table V, the same trend as in the day-ahead scheduling stage can be seen, as battery storage can help dispatch more wind generation; it decreases the total number of hours that slow and fast units are committed and reduces the system total costs. The security violations are also reduced, in general, for the cases with the battery. The results in Table V indicate that the cost savings are similar for the three lowest wind penetration levels, but lower for the 30% wind scenario. At 30% wind penetration level, the increase in the violation cost offsets the reduction in operating cost, which causes the system total cost for the 30% wind scenario to be higher than that of the 25% wind scenario. This is also a result due to out-of-sample testing, i.e., the stochastic program takes into consideration a subset of potential scenarios whereas the post-stage analysis tests the proposed solution against a wider range of potential scenarios.

Fig. 2 presents a boxplot of the total system costs for each case in the post-stage analysis. The edges of the box are the 25th and 75th percentiles and the whiskers represent the maximum and minimum without considering outliers. The horizontal red lines represent median values and outliers are shown in red “+”. The plot shows the median value as well as the variation in samples of system’s total costs for each case. The cases labeled “With x%” are the cases with the battery for “x%” wind penetration level; the rest are the cases without the battery. From Fig. 2, it can be noted that with the battery in the system, both the maximum and minimum value of the total system costs are reduced. Also, for wind penetration levels of 15%, 20% and 25%, the boxes for the cases with battery storage span much shorter ranges than those of the cases

without battery storage. This result indicates the variations of the total system costs are also lower for the cases with battery storage than those of the cases without battery storage if not considering the outliers (the red “+”). Though not shown, an ANOVA test was also conducted to confirm that the expected costs are significantly different between the two cases with and without battery storage.

TABLE IV. EXPECTED SYSTEM RESULTS FOR POST-STAGE ANALYSIS

Wind %	Involuntary Load Shedding (MWh)	Wind Curtailment (MWh)	Reserve Violations (MWh)	ETCH for Slow Units (h)	ETCH for Fast Units (h)
With Battery					
15%	0.0	0	4.0	297	145
20%	0.0	7	9.0	282	145
25%	0.4	130	9.9	272	140
30%	2.0	741	30.4	279	138
No Battery					
15%	0.0	0	5.1	367	146
20%	0.0	8	16.1	339	147
25%	0.0	124	22.4	321	147
30%	1.3	1009	31.0	313	147

TABLE V. EXPECTED SYSTEM TOTAL COSTS AND COST SAVINGS FOR POST-STAGE ANALYSIS

Wind %	Total Cost with Battery (\$)	Total Cost without Battery (\$)	Cost Savings (\$)	Cost Savings (%)
15%	847,874	971,823	123,948	12.8%
20%	827,291	943,955	116,664	12.4%
25%	808,768	936,378	127,610	13.6%
30%	876,424	957,140	80,715	8.4%

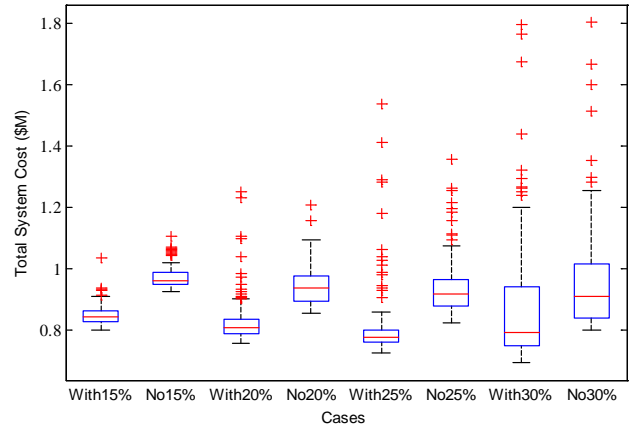


Fig. 2. Boxplot of total system costs for each case in the post-stage analysis.

Comparing the results for day-ahead scheduling to those for post-stage analysis, it can be observed that the cost savings by having battery storage in the system are lower in the post-stage analysis than those in the day-ahead scheduling. The reason is as follows. The post-stage analysis is formulated to approximate the real-time operation, where each dispatch problem is solved with limited foresight of future information (i.e. one hour look-ahead forecast) using a rolling horizon. When the realized wind generation deviates from the day-ahead forecast, the day-ahead battery schedule may not be able to address the unexpected deviation. Therefore, as shown in Table IV, the system reserve violations are higher in the

post-stage analysis than those in the day-ahead scheduling, especially at higher wind penetration levels. As the flexibility of the battery cannot be fully utilized with a fixed-schedule approach, reserve requirements are violated to ensure the feasibility of the problem. Therefore, as renewable penetration level increases, a more flexible operating approach is needed for battery storage.

It should be noted that this work simplifies the generation scheduling process adopted in industry today, where a short-term unit commitment is usually solved between the day-ahead scheduling stage and the real-time economic dispatch stage [36]. This is also one of the reasons that the benefit provided by the battery is lower in the post-stage analysis than that in the day-ahead scheduling. During such an intermediate stage, the day-ahead schedule for the battery could be updated based on the short-term wind forecast. Even though such a short-term unit commitment stage is not formulated in this paper, the two-step framework still captures the main challenges in scheduling battery storage in a system with increased uncertainties: 1) real-time operation has limited look-ahead functionalities and 2) the schedule obtained from a look-ahead scheduling process may not be able to fully utilize the flexibility of battery storage when uncertainties increase.

3) Cost-Benefit Analysis of the Battery

In this subsection, a cost-benefit analysis is performed to study if the cost savings achieved by using the battery can offset the investment cost of the battery. The cost-benefit analysis is performed using the results from the day-ahead stage for the 20% wind penetration level. The same cost-benefit analysis could also be done based on the real-time results from the post-stage analysis.

The day-ahead cost savings from six representative days are summarized in Table VI. The yearly total cost saving is computed using the cost savings from the six representative days. In Table VI, “D219” represents representative day 219 and similarly for the other representative days.

TABLE VI. SUMMARY OF DAY-AHEAD COST SAVINGS (\$K)

D219	D225	D230	D232	D236	D243	6-Day Sum	Yearly Sum
103	110	124	122	122	102	684	41619

As battery storage suffers from degradation effects, the impact of cycling on the life time of the battery should be taken into account. The expected daily and yearly discharging cycles are computed for the battery and summarized in Table VII. The daily expected discharging cycle is computed using (39). The maximum depth of discharge (DOD) of the battery is assumed to be 80%, since the battery has a minimum energy level of 30 MWh and a maximum energy capacity of 150 MWh. As shown in (39), the daily expected discharging cycle is calculated on an aggregated base. It is assumed in the cost-benefit analysis that the life time of the battery is sensitive only to the total number of equivalent full discharging cycles, i.e. the DOD of each discharging cycle has little to no effect on the life time of the battery. This is a reasonable assumption for some battery technologies [17], [34]. Since the initial SOC is required to be the same as the final SOC in the day-ahead UC, the number of daily equivalent full discharging cycles will be the same as the daily equivalent full charging cycles in

each scenario. Note that the energy used for deployment of spinning and regulation reserves is not counted in (39).

$$Daily_Discharge_Cycle = \pi_s \sum_s \frac{\sum_t P_{bst}^{out} / \eta_b^{out}}{E_b^{Max} - E_b^{Min}} \quad (39)$$

TABLE VII. EXPECTED DISCHARGING CYCLES FOR THE BATTERY

D219	D225	D230	D232	D236	D243	6-Day Sum	Yearly Sum
2.1	3.0	2.9	3.0	2.3	2.8	16.2	988.2

Assume the battery used in the study is a lithium-ion (Li-ion) battery. The cycle life for the battery is obtained from the DOE/EPRI energy storage handbook [33]. In [33], such batteries are assumed to last 15 years with a daily cycle, i.e. the total number of cycles is assumed to be $365 \times 15 = 5475$ cycles. Assuming the battery can be fully discharged at most 5475 cycles, the expected life time (number of years) in our analysis can be calculated using the expected yearly discharging cycles obtained from Table VII. Hence, the expected life time for the battery is calculated as

$$ExpLifeTime = \frac{5475}{988.2} \approx 5.5 \text{ Years.} \quad (40)$$

This result indicates that the battery is expected to last for about five and half years for the duty cycle in our case study. Assume the yearly cost saving obtained by using the battery is the same for the five and half years and that the discount factor is 6% per year. The present value, PV , of the system cost saving over this period is computed as

$$PV = \sum_t \frac{yearly_cost_saving}{(1+i_d)^t} = 191,387,407 (\$). \quad (41)$$

A wide range of cost estimates exist for Li-ion batteries [33]-[35]. In [33]-[35], the capital costs for batteries are calculated with the assumption of a specific battery technology and a specific configuration of the battery (power rating and energy capacity). In the paper, we assumed a capital cost, CC , of 3,000 \$/kW for the battery. This number is estimated based on the capital costs for Li-ion batteries with similar power ratings and energy capacities that reported in [33]-[35]. With a capital cost of 3,000 \$/kW, the net present value, NPV , of the battery is calculated as shown in (42):

$$NPV = PV - CC = 191,387,407 - 150,000,000 = 41,387,407 (\$) \quad (42)$$

We also calculate the breakeven cost for the battery, i.e. the capital cost that would give a zero NPV . The breakeven cost is found to be 3,828 \$/kW. The breakeven cost of the battery is plotted versus different values of discount factors in Fig. 3: it ranges from about 3,943 \$/kW to 3,612 \$/kW when the value of discount factor is selected in the range of 0.05 to 0.08.

The results of the cost-benefit analysis indicate that battery storage is beneficial to this system when current capital cost estimates, the degradation effect and its impact on the lifetime of the battery, are considered. However, it should be noted that as the costs for batteries vary depending on the battery configuration and technology, the conclusion may not apply to all battery storage technologies. Moreover, the estimated benefits only apply to the specific test power system, which is small and has high fuel costs. Larger systems with lower fuel costs are likely to see lower benefits of energy storage.

However, with that being said, the study in this section provides an adequate analysis to demonstrate the benefits and the cost-effectiveness of battery storage in systems with renewable resources. As the cost of battery storage is expected to be further reduced in the next five to ten years [2], the benefits of battery storage will be more prominent in the future.

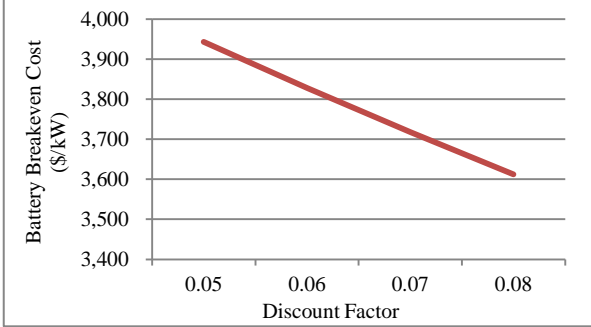


Fig. 3. Battery breakeven costs versus discount factor used in the cost-benefit analysis.

B. Evaluation of the Proposed Flexible Operating Range

To better utilize the flexibility of battery storage in systems with increased renewable resources, the flexible operating range approach is proposed. In this subsection, the performance of the proposed method is compared with the other three benchmark methods. The first benchmark compared is the fixed-schedule approach, presented in Section II. C. The second benchmark is referred to as the no-schedule approach. In the no-schedule approach, no predetermined schedule is provided for the battery. The dispatch of the battery in each time period is only based on the system condition in time period t and $t+1$. The decisions made in time period t do not take into account any forecast information beyond time period $t+1$. The third benchmark is referred to as the 3-hour look-ahead benchmark. In this benchmark, similar to the no-schedule benchmark, no schedule is provided for the battery. However, different from the no-schedule benchmark, the 3-hour look-ahead benchmark includes a look-ahead horizon of three hours, instead of the one hour modeled in the other benchmarks. A persistence wind power forecast is assumed, i.e. the wind generation in the look-ahead hours is the same as the wind generation in the current hour. For the no-schedule benchmark and the 3-hour look-ahead benchmark, the model described in Section II. B is used.

The performance of the four approaches is evaluated using wind scenarios for six days in 2012. For each representative day, the day-ahead stochastic UC is solved and the hourly-dispatch problem is solved with 150 different wind scenarios. The generator commitment schedules for slow units used in the three approaches are the same. The expected cost savings in percentage for the proposed approach to the benchmark methods are presented in Fig. 4 to Fig. 6 respectively.

As shown in Fig. 4, compared to the fixed-schedule benchmark, the proposed approach can provide about 1% to 3% cost savings for most of the cases. The cost savings tend to be larger at higher wind penetration levels than those for the 15% penetration level. This is because as wind penetration level increases, the intermittency in wind generation increases

in terms of MWs. Therefore, at higher wind levels, with the proposed approach, the battery can be used to compensate for the deviation in wind generation and provide more cost savings. In Fig. 4, there is only one case (D225, 15%) in which the performance of the proposed method is worse than the fixed-schedule case; and the cost difference is about 1%. The cause of the cost degradation in the case of (D225, 15%) is explained as follows. For day 225, at the day-ahead stage, the battery is scheduled to provide a large amount of spinning reserves in some time periods when wind generation suddenly decreases. As wind generation in the post-stage scenarios also has a large decrease in the same time periods as that in the day-ahead stage, no reserve violation occurs in the cases where the fixed-schedule approach is used; since the fixed-schedule approach implements the schedule determined at the day-ahead stage and can hence “anticipate” the sudden drop in wind generation. However, for the proposed approach, as it cannot fully “anticipate” the occurrence of large wind generation deviations, the battery may have been over utilized during prior time periods and thus does not have enough capability to provide the required amount of spinning reserves in those time periods. To further evaluate the performance of the proposed approach, in Table VIII, the six-day cost savings of the proposed approach compared to the fixed-schedule approach for the 15% wind penetration level is presented. As shown in Table VIII, the proposed approach can provide a six-day total cost saving of 34,273 dollars, or 1.1%. This result indicates that even though the proposed approach may be outperformed by the fixed-schedule approach in some cases, the proposed approach is more effective than the fixed-schedule approach overall.

Compared with the no-schedule method, the costs savings provided by the proposed method are higher than those of the fixed-schedule. This is in consistence with our intuition, since the no-schedule method does not account for future uncertainties when making decisions for the battery in each time period. The high cost saving shown in Fig. 5 is a result of the high security violations in the no-schedule case and the high penalty prices used in the simulation, since again, the decisions in the no-schedule benchmark are made based on only the current operating condition. In Fig. 6, the cost savings compared to the 3-hour look-ahead benchmark is presented. It can be seen from Fig. 6 that except for two cases, the proposed approach have better performance than the 3-hour look-ahead approach. Of course, the look-ahead approach would yield better results if a better forecast was used than persistence. But still, the result has demonstrated the effectiveness of the proposed approach in utilizing the flexibility of battery storage. In fact, the proposed approach could also be improved by utilizing a longer look-ahead horizon.

In Fig. 7, the result for day 236, scenario 3 with 30% wind penetration level is presented. The dashed lines in Fig. 7 represent the operating range determined by the proposed method, which is modeled as a pair of limits on the SOC of the battery. The red solid line (with square markers) shows the schedule obtained by the proposed approach. The blue solid line (with triangle markers) represents the schedule obtained by the fixed-schedule method. In Fig. 7, for the time periods in which the SOC of the battery is outside the limits, such as hour 20, 21 and 22, the SOC limits are relaxed by incurring

the penalty cost. For most of the time periods, the battery is operated within the range provided by the proposed method. As the flexible operating range is obtained using the day-ahead schedules, it provides a policy for the battery of when to discharge and charge. As shown in Fig. 7, the battery is forced by the limits to increase its SOC level during hours 10 to 13, and to decrease its SOC level during hours 14 to 15. Compared with the fixed-schedule approach, the proposed method can provide an operating range for the battery in each time period rather than a fixed operating point. As renewable generation deviates from forecasts, the battery is allowed to be operated within the operating range, and even possibly exceed the range, to compensate for the uncertainties in renewable generation. By using the proposed approach, the flexibility of the battery storage can be better utilized to address the intermittency in renewable resources.

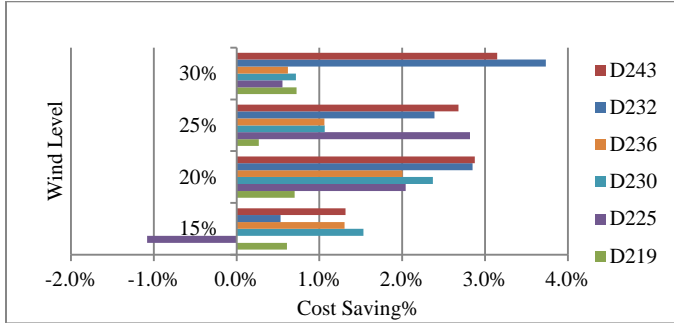


Fig. 4. Cost savings in percentage of the proposed method to the fixed-schedule method.

TABLE VIII. SIX-DAY COST SAVINGS OF THE PROPOSED METHOD COMPARED TO THE FIXED-SCHEDULE METHOD FOR 15% WIND PENETRATION

D219	D225	D230	D232	D236	D243	6-Day Sum (\$)	6-Day Sum (%)
4,584	-8,000	12,024	11,054	4,277	10,333	34,273	1.1%

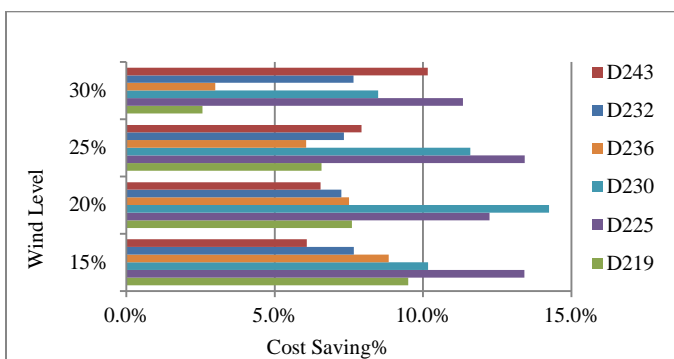


Fig. 5. Cost savings in percentage of the proposed method to the no-schedule method.

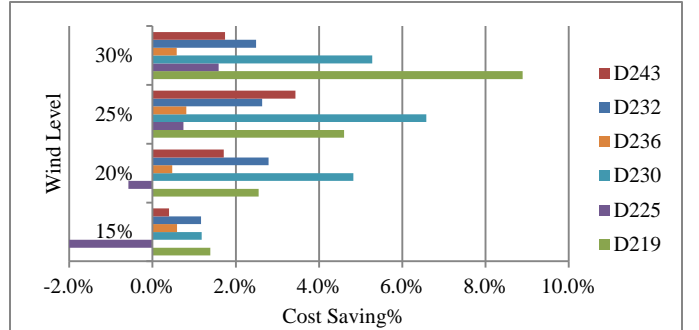


Fig. 6. Cost savings in percentage of the proposed method to the 3-hour lookahead method.

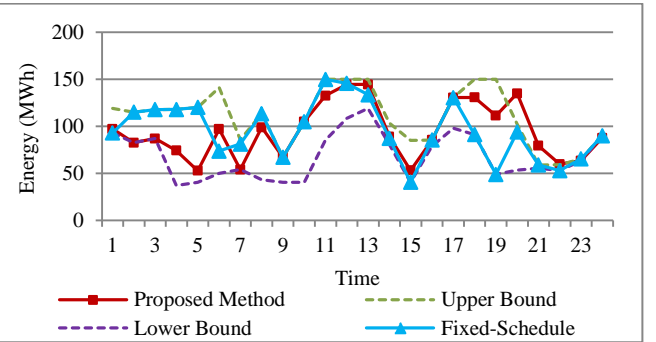


Fig. 7. Illustration of the proposed flexible operating range approach (Day 236, scenario 3, 30% wind level).

In Fig. 8, the energy and ancillary services scheduled for the battery for day 236, scenario 3 with 30% wind level are presented. The blue solid bars in Fig. 8 represent the power output of the battery, where positive value indicates discharging and negative value indicates charging. From Fig. 8, it can be seen that the battery is scheduled mainly to provide ancillary services, which is because of its fast-ramping capability. Also, it can be noted from Fig. 8 that the ancillary services provided by the battery are sometimes larger than its maximum power rating of 50 MW. This result occurs because the battery requires a short transition time between charging and discharging mode. In charging mode, a battery can stop charging and transition to discharging mode to provide up reserves. The maximum up reserve that the battery can provide in this case is $P_{bst}^{in} + P_{bt}^{out_max}$. This result suggests that the flexibility of battery storage will be more valuable when providing ancillary services.

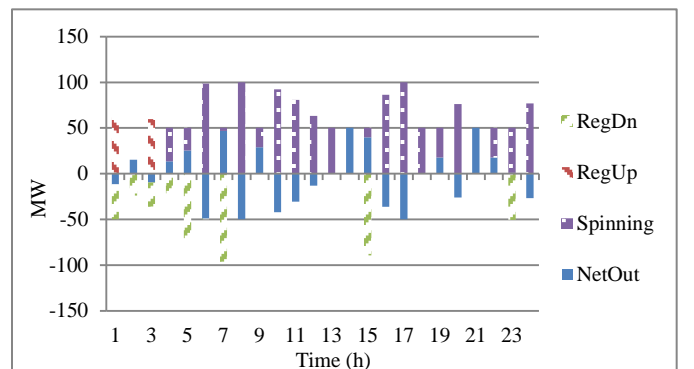


Fig. 8. Schedule for the battery using the proposed method (Day 236, scenario 3, 30% wind level).

IV. CONCLUSION

With its energy shifting and fast-ramping capabilities, battery storage has a great potential to facilitate the integration of high levels of renewable resources. In this paper, a two-step framework is used to evaluate the benefits of battery storage in power system operation with renewable resources. In the day-ahead scheduling stage, it is shown that battery storage can decrease the curtailment of wind generation, reduce load and reserve shortfalls as well as the commitment of thermal units, and lower the total system costs. Moreover, the cost-benefit analysis indicates that battery storage is a cost-effective solution. In the post-stage analysis, the challenge with operating a battery in real-time with limited look-ahead functionality is illustrated. The result in the post-stage analysis shows that using a fixed-schedule approach cannot make full use of the flexibility of the battery in real-time operation. To address this problem, we propose a flexible operating range approach for battery storage. The case study demonstrates that the proposed approach is more effective in operating battery storage in real-time dispatch compared to the fixed-schedule, no-schedule, and look-ahead benchmark methods. The proposed flexible operating range method is able to take advantage of the flexibility of energy storage to provide more cost savings compared with the other benchmark methods.

Directions for future work include the investigation of a wider set of strategies for real-time battery storage operations, possibly based on the marginal value or opportunity cost of using the battery for a given SOC. Moreover, we plan to develop a more detailed representation of the electrochemistry characteristic in battery storage, e.g. to capture how power limits and losses may depend on the SOC, and also a more detailed representation of degradation and life-time impacts of the battery under different operational schemes.

V. REFERENCES

- [1] M. Kintner-Meyer, *et al.*, "Energy storage for power system applications: a regional assessment for the northwest power pool," PNNL, Richland, WA. Apr. 2010. [Online]. Available: http://www.pnl.gov/main/publications/external/technical_reports/PNNL-19300.pdf.
- [2] DOE, "DOE energy innovation hub – batteries and energy storage," Mar. 2013. [Online]. Available: http://science.energy.gov/~/media/bes/pdf/hubs/JCESR_Fact_Sheet.pdf.
- [3] A. Tuohy and M. O'Malley, "Pumped hydro storage in systems with very high wind penetration," *Energy Policy*, vol. 39, no. 4, pp. 1965-1974, Apr. 2011.
- [4] M. Black and G. Strbac, "Value of bulk energy storage for managing wind power fluctuations," *IEEE Trans. Energy Convers.*, vol. 1, no. 1, pp. 197-195, Mar. 2007.
- [5] D. Pudjianto, M. Aunedi, P. Djapic, and G. Strbac, "Whole-systems assessment of the value of energy storage in low-carbon electricity systems," *IEEE Trans. Smart Grid*, vol. 5, no. 2, pp. 1098-1109, Mar. 2014.
- [6] H. Su and A. E. Gamal, "Modeling and analysis of the role of energy storage for renewable integration: power balancing," *IEEE Trans. Power Syst.*, vol. 28, no. 4, pp. 4109-4117, Nov. 2013.
- [7] N. Li and K. Hedman, "Economic Assessment of Energy Storage in Systems with High Levels of Renewable Resources," *IEEE Trans. Sustain. Energy*, vol. 6, no. 3, pp. 1103-1111, Jul. 2015.
- [8] D. J. Swider, "Compressed air energy storage in an electricity system with significant wind power generation," *IEEE Trans. Energy Convers.*, vol. 22, no. 1, pp. 95-102, Mar. 2007.
- [9] H. Daneshi and A. K. Srivastava, "Impact of battery energy storage on power system with high wind penetration," *IEEE Transm. and Dist. Conf. and Expo.*, May 2012.
- [10] B. Lu and M. Shahidehpour, "Short-term scheduling of battery in a grid-connected PV/battery system," *IEEE Trans. Power Syst.*, vol. 20, no. 20, pp. 1053-1061, May 2005.
- [11] T. Logenthiran and D. Srinivasan, "Short term generation scheduling of a microgrid," *IEEE Region 10 Conference*, Jan. 2009.
- [12] S. X. Chen, H. B. Gooi, and M. Q. Wang, "Sizing of energy storage for microgrids," *IEEE Trans. Smart Grid*, vol. 3, no. 1, pp. 142-151, Mar. 2012.
- [13] C. Uckun, A. Botterud, and J. Birge, "An improved stochastic unit commitment formulation to accommodate wind power," *IEEE Trans. Power Syst.*, accepted for publication.
- [14] H. Mohsenian-Rad, "Coordinated price-maker operation of large energy storage units in nodal energy markets," *IEEE Trans. Power Syst.*, accepted for publication.
- [15] H. Mohsenian-Rad, "Optimal bidding, scheduling, and deployment of battery systems in California day-ahead energy market," *IEEE Trans. Power Syst.*, accepted for publication.
- [16] D. Pozo, J. Contreras, and E. E. Sauma, "Unit commitment with ideal and generic energy storage units," *IEEE Trans. Power Syst.*, vol. 29, no. 6, pp. 2974-2984, Oct. 2014.
- [17] M. A. Ortega-Vazquez, "Optimal scheduling of electric vehicle charging and vehicle-to-grid services at household level including battery degradation and price uncertainty," *IET Generation, Transmission & Distribution*, vol. 8, no. 6, pp. 1007-1016, Jun. 2014.
- [18] W. B. Powell and S. Meisel, "Tutorial on stochastic optimization in energy—part II: an energy storage illustration," *IEEE Trans. Power Syst.*, accepted for publication.
- [19] D. F. Salas and W. B. Powell, "Benchmarking a scalable approximate dynamic programming algorithm for stochastic control of multidimensional energy storage problems," Department of Operations Research and Financial Engineering, Princeton Univ., Princeton, NJ, USA, Tech. Rep. 2004, 2015. [Online]. Available: <http://castelab.princeton.edu/Papers/Salas%20Powell%20-Benchmarking%20ADP%20for%20multidimensional%20energy%20storage%20problems.pdf>
- [20] J. H. Kim and W. B. Powell, "Optimal energy commitments and intermittent supply," *Operation Research*, vol. 59, no. 6, pp. 1347-1360, Nov. 2011.
- [21] C. Goebel, D. S. Callaway, and H. A. Jacobsen, "The impact of state of charge management when providing regulation power with energy storage," *IEEE Trans. Power Syst.*, vol. 29, no. 3, pp. 1433-1434, Apr. 2014.
- [22] A. Papavasiliou, S. S. Oren, and R. P. O'Neil, "Reserve requirements for wind power integration: a scenario-based stochastic programming framework," *IEEE Trans. Power Syst.*, vol. 26, no. 4, pp. 2197-2206, Nov. 2011.
- [23] M. L. Stein., *Interpolation of Spatial Data: Some Theory for Kriging*. Berlin: Springer Verlag, 1999.
- [24] W. Skamarock, J. B. Klemp, J. Dudhia, D. O. Gill, D. M. Barker, M. G. Duda, X. Y. Huang, W. Wang, and J. G. Powers, "A description of the advanced research WRF version 3," NCAR, Boulder, CO. Jun. 2008. [Online]. Available: http://www2.mmm.ucar.edu/wrf/users/docs/arw_v3.pdf
- [25] E. M. Constantinescu, V. M. Zavala, M. Rocklin, S. Lee, and M. Anitescu, "A computational framework for uncertainty quantification and stochastic optimization in unit commitment with wind power generation," *IEEE Trans Power Syst.*, vol. 26, no. 1, pp. 431-441, Feb. 2011.
- [26] J. Dupacová, N. Gröwe-Kuska, and W. Römisch, "Scenario reduction in stochastic programming: An approach using probability metrics," *Math. Program, Series A*, vol. 3, pp. 493-511, Feb. 2003.
- [27] University of Washington, "Power systems test case archive," Dept. Elect. Eng., 1999. [Online]. Available: http://www.ee.washington.edu/research/pstca/pts/pg_tcharts.htm
- [28] J. M. S. Pinheiro, C. R. R. Dornellas, M. Th. Schilling, A. C. G. Melo, and J. C. O. Mello, "Probing the new IEEE reliability test system (RTS-96): HL-II Assessment," *IEEE Trans. Power Syst.*, vol. 13, no. 1, pp. 171-176, Feb. 1998.
- [29] J. D. Lyon, F. Wang, K. W. Hedman, and M. Zhang, "Market implications and pricing of dynamic reserve policies for systems with renewables," *IEEE Trans. Power Syst.*, accepted for vol. 30, no. 3, pp. 1593-1602, May 2015.
- [30] DOE Global Energy storage Database, "Duke Energy Notrees wind storage demonstration project," [Online]. Available: <http://www.energystorageexchange.org/projects/11>

- [31] DOE Global Energy storage Database, "Rokkasho village wind farm," [Online]. Available: <http://www.energystorageexchange.org/projects/385>
- [32] DOE Global Energy storage Database, "ASE Larurel Mountain," [Online]. Available: <http://www.energystorageexchange.org/projects/164>
- [33] Sandia National Laboratories, "DOE/EPRI 2013 electricity storage handbook in collaboration with NEECA," Jul. 2013. [Online]. Available: <http://energy.gov/oe/downloads/doeepri-2013-electricity-storage-handbook-collaboration-neca-july-2013>
- [34] International Renewable Energy Agency, "Battery storage for renewables: market status and technology outlook," Jan. 2015. [Online]. Available: http://www.irena.org/DocumentDownloads/Publications/IRENA_Battery_Storage_report_2015.pdf
- [35] Electric Power Research Institute, "Cost-effectiveness of energy storage in California," Jun. 2013. [Online]. Available: http://www.cpuc.ca.gov/NR/rdonlyres/1110403D-85B2-4FDB-B927-5F2EE9507FCA/0/Storage_CostEffectivenessReport_EPRI.pdf
- [36] California ISO, "Market process," [Online]. Available: <http://www.caiso.com/market/Pages/MarketProcesses.aspx>

Nan Li (S'11) received the B.E. degree in electrical engineering from North China Electric Power University, in Beijing, China and the M.S. degree in electrical engineering from Arizona State University, Tempe, AZ, in 2010, and 2012 respectively. Currently, he is pursuing the Ph.D. degree in electrical engineering from Arizona State University, Tempe, AZ. His research interests include power system economics, operations, energy storage, and the application of data science in power system.

Canan Uçkun received the B.Sc. degree in industrial engineering from Marmara University in 2003, the M.Sc. degree in industrial engineering from Koç University, Istanbul, Turkey, in 2006, and the Ph.D. degree in operations management/management science from the University of Chicago, Booth School of Business, in 2012. She is a Researcher in Engineering Systems Modeling in the Center for Energy, Environmental, and Economic Systems Analysis (CEES) at Argonne National Laboratory, Argonne, IL, USA. She has done research on electricity markets, smart grid, demand response, revenue management, and inventory systems. Her current work includes stochastic unit commitment, renewable integration, grid-level energy storage, and demand response related projects.

John R. Birge received the A.B. degree in mathematics from Princeton University, Princeton, NJ, USA, and the M.S. and Ph.D. degrees in operations research from Stanford University, Stanford, CA, USA. He is currently the Jerry W. and Carol Lee Levin Professor of Operations Management at the University of Chicago Booth School of Business. Previously, he was Dean of the McCormick School of Engineering and Applied Science and Professor of Industrial Engineering and Management Sciences at Northwestern University from 1999 to 2004. He also served as Professor and Chair of Industrial and Operations Engineering at the University of Michigan, where he was from 1980 to 1999, as Vice-Chair of the University of Michigan Senate Assembly,

and as Vice President-Subdivisions and President of the Institute for Operations Research and the Management Sciences (INFORMS). Prof. Birge is former Editor-in-Chief of *Mathematical Programming, Series B*. He also serves on the editorial boards of *Mathematical Programming, Series A*, *Operations Research*, *Management Science*, *Interfaces*, *Naval ResearchLogistics*, *Computational Optimization and Applications*, and *Management Science*. He chaired the Fifth International Conference on Stochastic Programming in 1989, the XV International Symposium on Mathematical Programming in 1994, and the XX International Symposium on Mathematical Programming in 2009. He was selected as an Office of Naval Research Young Investigator in 1986 and received the Medallion Award from the Institute of Industrial Engineers in 2002, the Fellows Award from INFORMS in 2002, the George Kimball Prize from INFORMS in 2008, and the Distinguished Fellow Award from the Manufacturing and Service Operations Management Society (MSOM) in 2013. In 2011, he was elected a member of the National Academy of Engineering.

Emil M. Constantinescu received his Ph.D. degree in Computer Science from Virginia Tech, Blacksburg, in 2008. He is currently a Computational Mathematician in the Mathematics and Computer Science Division at Argonne National Laboratory, Argonne, IL. His research interests include uncertainty quantification in weather and climate models and their applications to energy systems.

Kory W. Hedman (S'05, M'10) received the B.S. degree in electrical engineering and the B.S. degree in economics from the University of Washington, Seattle, in 2004 and the M.S. degree in economics and the M.S. degree in electrical engineering from Iowa State University, Ames, in 2006 and 2007, respectively. He received the M.S. and Ph.D. degrees in industrial engineering and operations research from the University of California, Berkeley in 2008 and 2010 respectively.

Currently, he is an assistant professor in the School of Electrical, Computer, and Energy Engineering at Arizona State University. He previously worked for the California ISO, Folsom, CA and he has worked for the Federal Energy Regulatory Commission, Washington, DC. His research interests include power systems operations and planning, power systems economics, operations research, stochastic programming, and market design.

Audun Botterud (M'04) received the M.Sc. degree in industrial engineering and the Ph.D. degree in electrical power engineering from the Norwegian University of Science and Technology, Trondheim, Norway, in 1997 and 2004, respectively. He is a Principal Energy Systems Engineer in CEEES at Argonne National Laboratory, Argonne, IL, USA. He was previously with SINTEF Energy Research in Trondheim, Norway. His research interests include power systems planning and economics, electricity markets, grid integration of renewable energy, energy storage, and stochastic optimization. Dr. Botterud is co-chair for the IEEE Task Force on Bulk Power System Operations with Variable Generation.